WATER RESOURCES RESEARCH, VOL. 33, NO. 12, PAGES 2759–2767, DECEMBER 1997

Two-phase flow infiltration equations accounting for air entrapment effects

Zhi Wang and Jan Feyen
Institute for Land and Water Management, Katholieke Universiteit Leuven, Leuven, Belgium

Donald R. Nielsen
Department of Land, Air, and Water Resources, University of California, Davis

Martinus T. van Genuchten
U.S. Salinity Laboratory, USDA-ARS, Riverside, California

Abstract. Water infiltration into the unsaturated zone is potentially affected by air compression ahead of the wetting front. Analytical infiltration equations accounting for air compression, air counterflow, and flow hysteresis in a porous medium were derived on the basis of the *Green and Ampt* [1911] assumptions. Air compression ahead of the wetting front was predicted using the perfect gas law. The capillary pressure at the wetting front was found to vary between the dynamic water-bubbling value and the dynamic air-bubbling value of the material. These equations, accounting also for the effects of macropores near the soil surface, turned out to be simpler than the traditional *Kostiakov* [1932] and the *Philip* [1957a, b, c, d] equations. The equation parameters are physically meaningful and can be readily obtained from field measurements of the natural saturated hydraulic conductivity and soil water retention or pressure infiltrometer data. Experimental testing showed that the equations are reasonably accurate.

1. Introduction

The effects of air confinement ahead of the wetting front on water infiltration into unsaturated soils have been studied by many earlier investigators [e.g., *Green and Ampt*, 1911; *Kostiakov*, 1932; *Powers*, 1934; *Christiansen* 1944]. *Philip* [1957a, b, c, d] and *Parlange* [1971, 1975a, b] contributed major theoretical analyses of infiltration based on soil water diffusion properties. Their studies were mostly based on the assumption that the air displaced by the infiltrating water escapes so readily that the pressure of the soil air is atmospheric [*Philip*, 1957c]. By contrast, the more realistic case, when air is not free to escape, was considered to be too difficult for mathematical treatment and remains largely unsolved [*Philip*, 1993]. Since air entrapment effects on infiltration properties were found to be significant in a number of laboratory and field experiments [e.g., *Wilson and Luthin*, 1963; *Youngs and Peck*, 1964; *Peck*, 1965a, b; *Adrian and Franzini*, 1966; *McWhorter*, 1971; *Smiles et al*., 1971; *Dixon and Linden*, 1972; *Vachaud et al*., 1973, 1974; *Watson and Curtis*, 1979; *Touma et al*., 1984; *Grismer et al*., 1994; *Latifi et al*., 1994; *Wang et al*., 1997], many investigators have attempted to derive analytical and numerical models accounting for the air effects [e.g., *Brustkern and Morel-Seytoux*, 1970, 1975; *McWhorter*, 1971; *Noblanc and Morel-Seytoux*, 1972; *Morel-Seytoux and Khanji*, 1974, 1975; *Sonu and Morel-Seytoux*, 1976; *Parlange and Hill*, 1979; *Touma et al*., 1984; *Morel-Seytoux and Billica*, 1985a, b; *Sander et al*., 1988; *Felton and Reddell*, 1992]. Although these models were successful in explaining some of the experimental findings, the complex and nonlinear relations describing water infiltration into the air-confining vadose zone are still not fully understood. For example, the effects of air pressure fluctuation, air eruptions from the surface, hysteresis in capillary pressure, and macropores on infiltration have not been systematically studied and incorporated into previous models. The effects of air entrapment on water flow may be described using a complete two-phase diffusion-type approach involving a set of coupled Richards' equations [*Touma et al*., 1984; *Morel-Seytoux and Billica*, 1985a, b; *Sander et al*., 1988] or by means of more approximate flow descriptions that invoke such simplifications as first suggested by *Green and Ampt* [1911]. *Whisler and Bouwer* [1970] previously compared several methods for calculating water infiltration into soils and concluded that a numerical analysis of diffusion models gave the best agreement with observations but required a considerable amount of input data (hydraulic functions that are not readily available from the field) and the calculation procedure itself was not simple, whereas the piston-type Green and Ampt infiltration equation was the easiest to use, gave reasonably accurate results, and was still the most usable model for practical field problems. Piston-type models can give reasonable estimates of the depth of wetting, the infiltration capacity, and the cumulative depth of water infiltration with readily available input parameters but may not be able to accurately reproduce actual water content/pressure profiles as a function of time or space.

The objectives of this study are (1) to present a simple set of a two-phased *Green and Ampt* [1911] model accounting for air compression and dynamic change of capillary pressure at the wetting front, (2) to derive a set of analytical infiltration equations accounting for air compression, air pressure fluctuation/air eruption, flow hysteresis, and macropores in a porous

Paper number 97WR01708.
0043-1397/97/97WR-01708$09.00

medium, and (3) to validate these equations using column experimental data.

2. Theoretical Development

2.1. Analysis of the Green and Ampt Equation

Extending the *Green and Ampt* [1911] analogy for flow in a capillary tube to soil medium, the rate of water infiltration is approximately given as

$$i_w = -K_s \frac{dH_w}{dz} = -K_s \frac{(h_{wf} - z) - h_0}{z} = K_s \frac{h_0 + z - h_{wf}}{z} \tag{1}$$

where i_w is the rate of water infiltration, K_s is the saturated hydraulic conductivity at the residual nonwetting fluid (air) saturation [*Bouwer*, 1964; *Morel-Seytoux and Khanji*, 1974], dH_w/dz is the gradient of total water head H_w, h_{wf} is the gage soil water pressure head at the wetting front, z is the wetting depth (positive downward), and h_0 is the water pressure head at the soil surface.

The capillary pressure (or soil suction head for water) at the wetting front is generally determined by $h_{cf} = h_{af} - h_{wf}$ [*Morel-Seytoux*, 1973], where h_{af} is the air pressure immediately below the wetting front and h_{wf} is the water pressure immediately above the wetting front (in excess of atmospheric pressure). Writing the water head in (1) as $h_{wf} = h_{af} - h_{cf}$ results in the general infiltration equation

$$i_w = K_s \frac{h_0 + h_{cf} - h_{af} + z}{z} \tag{2}$$

which is of the type proposed by *Green and Ampt* [1911] except for the inclusion of the gage air pressure, h_{af}. Calculations of i_w using (2) require an estimate of the effective capillary pressure head h_{cf} at the wetting front, which is a parameter that can vary significantly across the wetting front. An earlier mechanistic analysis of h_{cf} based on an analysis of soil water retention curve (SWRC) was provided by *Youngs and Peck* [1964]. They wrote that "initially upon infiltration, the soil surface immediately wets to saturation following the main wetting curves of the porous medium. As the material takes up water, the air pressure h_{af} increases and the capillary pressure at the soil surface follows the main draining curve until the air entry value is reached and soil air escapes from the soil surface" (p. 2). *Peck* [1965b] further speculated that the gage air pressure required to initiate the air escape can be expected to be equal to the water pressure at the bottom depth of the saturated zone plus the air entry pressure of the material. Air escape would cease when the pressure reaches a value "low enough but not zero" to allow the air escape route to be sealed by effective saturation, at which time h_{af} starts to increase again with further water uptake. Subsequently, the material drains following a secondary scanning curve which does not start from $h_{cf} = 0$. In a recent experiment [*Wang et al*., 1997] we confirmed Peck's speculation and determined the two extreme air pressures with relation to water flow hysteresis in a porous medium. The maximum h_{af} at the time when air erupts from the soil surface was called the "air-breaking value," H_b, defined by

$$H_b = h_0 + z + h_{ab} \tag{3}$$

where h_{ab} is the air-bubbling capillary pressure value of the material and z is the wetting depth (or the minimum wetting depth if the wetting front is not sharp). The minimum "low enough but not zero" h_{af} immediately after air escape was called the "air-closing value," H_c, defined by

$$H_c = h_0 + z + h_{wb} \tag{4}$$

where h_{wb} is the water-bubbling value of the material (a positive quantity). According to (3) and (4), the capillary pressure at the wetting front varies dynamically from the water-bubbling pressure, $h_{cf} = h_{wb}$ when $h_{af} \le H_c$ to the air-bubbling pressure $h_{cf} = h_{ab}$ at $h_{af} = H_b$. When h_{af} increases from H_c to H_b, h_{cf} also increases following a scanning drainage curve toward the inflection point on the main drainage curve. Inversely, when h_{af} decreases from H_b to H_c, h_{cf} decreases following a scanning wetting curve toward the inflection point on the main wetting curve [*Wang et al*., 1997].

Values of h_{ab} and h_{wb} in (3) and (4) are mathematically defined at the inflection points $d^2S_w/dh_c^2 = 0$ of the main drainage and the wetting curves of the material, respectively. Assuming applicability of *van Genuchten*'s [1980] model for the soil water retention curve, the inflection capillary pressure head, h_c^*, is given by

$$\begin{aligned} h_c^* &= \frac{1}{\alpha}\left[\frac{n-1}{n(m+1)-n+1}\right]^{1/n} = \frac{1}{\alpha} m^{1/n} \qquad m = 1 - 1/n \\ h_c^* &= \frac{1}{\alpha}\left[\frac{n-1}{n(m+1)-n+1}\right]^{1/n} = \frac{1}{\alpha} \qquad m = 1 - 2/n \end{aligned} \tag{5a}$$

and the corresponding inflection water saturation, S_w^*, by

$$\begin{aligned} S_e^* &= \left[1 - \frac{n-1}{n(m+1)}\right]^m = \left(\frac{1}{1+m}\right)^m \qquad m = 1 - 1/n \\ S_e^* &= \left[1 - \frac{n-1}{n(m+1)}\right]^m = 0.5^m \qquad m = 1 - 2/n \end{aligned} \tag{5b}$$

where α, m, and n are parameters. Because of the dynamic effects of moving water and air on a SWRC [*Corey and Brooks*, 1975] during infiltration, we suggest that h_{ab} and h_{wb} be evaluated at $h_{ab} = 1/\alpha_d$ and $h_{wb} = 1/\alpha_w - \delta = h_{ab}/2 - \delta$ cm ($\delta = 0 \sim 2$ for sandy soils; $\delta = 2 \sim 5$ for loamy soils and $\delta = 8 \sim 10$ for clay soils), where the subscripts d and w denote the main drainage curve and the main wetting curve, respectively. According to information provided by *Carsel and Parrish* [1988] and *van Genuchten et al*. [1991], the estimated dynamic values of h_{ab} and h_{wb} along with other parameters of 12 major soil texture groups are listed in Table 1. These parameters will be used in this study as a reference data set for various soils. Recent studies [*Fallow and Elrick*, 1996] also indicate that in situ estimates of h_{ab} and h_{wb} can be easily obtained using pressure infiltrometer method.

Other methods for estimating the wetting front suction have been proposed. The methods all assumed that this suction is a constant value for a certain medium. *Bouwer* [1964] proposed that h_{cf} in (2) can be replaced by a critical pressure head P_c defined by the conductivity weighted average value of the capillary pressure across the wetting retention curve as follows:

$$P_c = \frac{1}{K_s} \int_0^\infty K_{rw}\, dh_{cf} \tag{6}$$

where K_{rw} is the relative hydraulic conductivity, K/K_s. A close approximation of (6) for *van Genuchten* [1980] hydraulic properties was recently given by *Morel-Seytoux et al*. [1996]:

Table 1. Hydraulic Parameters for 12 Major Soil Texture Groups

Soil Texture	θ_r, cm^3/cm^3	θ_s, cm^3/cm^3	α, cm^{-1}	n	h_{ab}, cm	h_{wb}, cm	K_s, cm/h	ϕ, cm^3/cm^3	$S_{w,0}$	$S_{nw,c}$
Silt clay	0.07	0.36	0.005	1.09	210	100	12	0.399	0.194	0.167
Clay	0.068	0.38	0.008	1.09	130	60	115	0.417	0.179	0.159
Silt clay loam	0.089	0.43	0.01	1.23	105	50	41	0.480	0.207	0.173
Silt	0.034	0.46	0.016	1.37	65	30	144	0.478	0.074	0.107
Clay loam	0.095	0.41	0.019	1.31	55	25	149	0.464	0.232	0.186
Silt loam	0.067	0.45	0.02	1.41	54	23	260	0.486	0.149	0.144
Sandy clay	0.1	0.38	0.027	1.23	40	17	70	0.438	0.263	0.202
Loam	0.078	0.43	0.036	1.56	30	12	600	0.473	0.181	0.161
Sandy clay loam	0.1	0.39	0.059	1.48	18	7	754	0.447	0.256	0.198
Sandy loam	0.065	0.41	0.075	1.89	14	6	2546	0.445	0.159	0.149
Loamy sand	0.057	0.41	0.124	2.28	9	4	8405	0.441	0.139	0.140
Sand	0.045	0.43	0.145	2.68	8	3	17107	0.454	0.105	0.122

After *Carsel and Parrish* [1988] *van Genuchten et al*. [1991].

$$P_c = \frac{0.046m + 2.07m^2 + 19.5m^3}{\alpha(1 + 4.7m + 16m^2)} \tag{7}$$

Whisler and Bouwer [1970] suggested that h_{cf} in (2) is the water entry pressure, h_{ce}, in the wetting retention model of *Brooks and Corey* [1966]. *Mein and Larson* [1973] used P_c instead of h_{ce}, whereas *Morel-Seytoux and Khanji* [1974] proposed a two-phase equation for the effective capillary drive, H_{ef}:

$$H_{ef} = \int f_w \, dh_c \tag{8}$$

where f_w was introduced as the fractional flow function accounting for the relative water conductivity, K_{rw}, and the relative air conductivity, K_{ra}. In addition to replacing h_{cf} in (2) by H_{ef}, K_s was replaced by K_s/β (where β is called the viscous resistance correction factor, varying in a range between 1.0 and 1.7). On the basis of the work of *Morel-Seytoux and Khanji* [1974], *Brakensiek* [1977] applied the Brooks and Corey model to the wetting retention curve and obtained the following simplified equation for the effective capillary pressure, S, of the wetting front

$$S = \frac{2 + 3\lambda}{1 + 3\lambda} h_{ce} \tag{9}$$

where λ is the pore size distribution index in the Brooks and Corey model. Brakensiek compared the results of (7), (8), and (9) and *Mein and Larson*'s [1973] approach using data of seven soils and concluded that all of the above procedures lead to very similar average h_{cf} values.

In view of the above physical and mathematical definitions, *Brakensiek*'s [1977] effective capillary pressure, *S, Bouwer*'s [1964] and *Mein and Larson*'s [1973] P_c, and *Morel-Seytoux and Khanji*'s [1974] H_{ef}, should be closest to the water-bubbling value, h_{wb}, as given by the inflection point of the wetting retention curve. By comparison, *Whisler and Bouwer*'s [1970] water entry pressure, h_{ce}, should be the smallest because of its association with natural saturation $S_e = 1$ (i.e., as extrapolated to saturation using the Brooks-Corey wetting retention model). Note that estimates of P_c, S, H_{ef}, and h_{ce} require at least one set of measured or estimated wetting retention data, which after all is not easily obtained. Alternatively, pressure infiltrometer methods [*Fallow and Elrick*, 1996] could be used to determine in situ dynamic estimates of h_{wb}, h_{ab}, and the natural saturated hydraulic conductivity [*Elrick and Reynolds*, 1992]. An advantage of pressure infiltrometer methods is that the relatively complicated and time-consuming experiments for the (static) wetting retention curves are no longer necessary.

2.2. Infiltration Without Air Compression

According to the previous discussion, when soil air is not compressed during infiltration ($h_{af} = 0$), $h_{cf} = h_{wb}$. Thus (2) can be rewritten as

$$i_w = K_s \frac{h_0 + h_{wb} + z}{z} \tag{10}$$

Integration of (10), assuming h_0 is constant, gives the time of infiltration at z:

$$t = \frac{\phi(1 - S_{w,0} - S_{nw,0})}{K_s} \cdot \left[z - (h_0 + h_{wb}) \ln\left(1 + \frac{z}{h_0 + h_{wb}}\right) \right] \tag{11}$$

where ϕ is the porosity of the porous medium, $S_{w,0}$ is the initial water saturation before infiltration, $S_{nw,0}$ is the saturation of the nonwetting fluid (air) in the wetted zone, and K_s the natural saturated water conductivity at $S_{nw,0}$ [*Morel-Seytoux*, 1973]. In field situations, K_s, ϕ, $S_{w,0}$, $S_{nw,0}$, and h_{wb} may all vary with z. When z is replaced by $I_w/[\phi(1 - S_{w,0} - S_{nw,0})]$, (10) and (11) show explicit relationships between the cumulative infiltration I_w and i_w and between I_w and t, respectively.

2.3. Infiltration With Air Compression and Air Counterflow

When water infiltrates through the soil surface over a large area, soil air initially at local barometric pressure, h_b ($\approx$10 m of water), is displaced and probably compressed ahead of the wetting front by the penetrating water. Assuming that the infiltration process is isothermal, the medium is homogeneous, and the wetting front is sharp, the soil air pressure, h_{af}, in excess of h_b is calculated from Boyle's law for a perfect gas as

$$h_{af} = h_b\left(\frac{z}{B - z}\right) \tag{12}$$

where z is the depth of wetting and B is the depth of air-flow barrier below the soil surface (e.g., an air-impermeable stratum or the groundwater table). When h_{af} is less than the air-closing value, $H_c = z + h_0 + h_{wb}$, the capillary pressure at the

wetting front is $h_{cf} = h_{wb}$. The conductivity to water is reduced to $K_c = k_{rc}K_s$, where k_{rc} is the relative water conductivity accounting for air-confining condition. Thus (2) becomes

$$i_w = K_c \frac{z + h_0 + h_{wb} - h_{af}}{z} \tag{13}$$

and the time t when the infiltration front reaches z is given by

$$t = \frac{1}{K_e} \cdot \left[z - (h_0 + h_{wb} - h_{af}) \ln \left(1 + \frac{z}{h_0 + h_{wb} - h_{af}} \right) \right] \tag{14}$$

where K_e is the effective conductivity defined by

$$K_e = \frac{K_c}{\phi(1 - S_{w,0} - S_{nw,c})} = \frac{k_{rc}K_s}{f} \tag{15}$$

$S_{nw,c}$ is the residual air entrapment under air-confining condition; k_{rc} and K_c are, respectively, the relative and the actual water conductivity corresponding to $S_{nw,c}$; and $f \equiv \phi(1 - S_{w,0} - S_{nw,c})$ is the effective porosity for the infiltrating flow (water). For simplicity of integration and calculation, h_{af} is assumed a constant. This assumption does not cause significant error when h_{af} calculated by (12) is directly substituted into (14) to determine the value of time t. Another integration of (13), assuming that z is small compared to the column depth, was given by *Morel-Seytoux and Khanji* [1974, equation (5)]. Notice that (10) and (11) are special cases of (13) and (14) when $h_{af} \equiv 0$.

Substituting (12) into (13) and solve for $i_w = 0$, the wetting depth, z_0, at $i_w = 0$, is given by

$$z_0 = \frac{1}{2}[(b^2 + 4a)^{1/2} - b] \tag{16}$$

where $a = B(h_0 + h_{wb})$ and $b = h_b + h_0 + h_{wb} - B$. The corresponding time, t_0, at the zero rate of infiltration can be approximated from (14) by letting $h_{af} \rightarrow h_0 + h_{wb}$, in which case

$$t_0 = \frac{z_0}{K_e} \tag{17}$$

Figure 1 depicts z_0 and t_0 values for the 12 major soil texture groups listed in Table 1. Notice that the values of z_0 and t_0 are very small for coarse-textured soils and/or when the air-barrier depth B is less than 10 m. However, for fine-textured soils and/or when $B > 10$ m, z_0 and t_0 become very large.

When h_{af} becomes greater than $H_c = z + h_0 + h_{wb}$, the interconnected large pores at the wetting front begin to desaturate even though the frontal micropores continue to take up water from the wetted layer. The average water saturation value at the wetting front, S_w, generally decreases. The corresponding value of h_{cf} automatically increases following a scanning drainage curve toward the inflection point on the main drainage curve. Eventually, the increment in h_{cf} equals that in h_{af}. Until the inflection point on the main drainage curve is reached, h_{af} equals the air-breaking value, $H_b = h_0 + z + h_{ab}$ and $h_{cf} = h_{ab}$. At this sufficiently high air pressure the entrapped soil air breaks through the interconnected large pores of the wetted zone and escapes from the soil surface. During the period when h_{af} increases from H_c to H_b, the infiltration rate i_w is identically zero as indicated by (2).

Immediately after air escapes from the soil surface, the value of h_{af} quickly decreases, as was noticed by *Peck* [1965b], *Grismer et al.* [1994], *Latifi et al.* [1994], and *Wang et al.* [1997]. Hence water begins then to resaturate the wetting front with h_{cf} decreasing toward h_{wb}. Because both the size of air channels and the value of air conductivity are much greater than those for water in a porous medium, the rate of resaturation, or the decrease in h_{cf}, is also much slower than the rate at which h_{af} decreases. When h_{af} drops to $H_c = z + h_0 + h_{wb}$, h_{cf} may have just started to decrease from h_{ab} to h_{wb} following a scanning wetting curve to the inflection point on the main wetting curve. It follows from (2) that during air eruption ($h_{cf} \approx h_{ab}$ and $h_{af} \approx h_0 + z + h_{wb}$), the rate of infiltration reaches a maximum value defined by

$$i_{\max} = K_c \frac{h_{ab} - h_{wb}}{z} \tag{18}$$

After air eruption, the air pressure in the soil becomes very low (but not zero) and the air-bubbling channels will become sealed by resaturation. At the air closing time, $h_{af} = h_0 + z + h_{wb}$ and $h_{cf} = h_{wb}$, and the water inflow rate attains the minimum potential rate, $i_{\min} \approx 0$. Subsequently, h_{af} and h_{cf} will increase again until a second air-breaking event occurs, followed by a second air-closing event. Assuming that this cyclic process will repeat itself during the remaining period of infiltration [*Wang et al.*, 1997], i_w will fluctuate between close to $i_{\max}$, defined by (18), and close to $i_{\min} = 0$. Assuming linearity, the rate of water infiltration after t_0 can be averaged as $i_w = (i_{\max} + i_{\min})/2$, or

$$i_w = \frac{K_c}{2} \frac{h_{ab} - h_{wb}}{z} \tag{19}$$

Note that i_w is now independent of h_0 and B. The time of infiltration after t_0 is given by

$$t = t_0 + \frac{(z^2 - z_0^2)}{K_e(h_{ab} - h_{wb})} \tag{20}$$

from which the z-t relation is

$$z = [z_0^2 + K_e(h_{ab} - h_{wb})(t - t_0)]^{1/2} \tag{21}$$

Combining (21) and (19) yields

$$i_w = \frac{K_c(h_{ab} - h_{wb})}{2} [z_0^2 + K_e(h_{ab} - h_{wb})(t - t_0)]^{-1/2} \tag{22}$$

which is an explicit form of the infiltration equation during periods of air counterflow. A complete set of equations for the entire period of infiltration hence consists of (13) and (14) for the first period when $t < t_0$, with air compression ahead of the wetting front, and (22) for the remaining periods when $t > t_0$, with air counterflow across the wetted layers.

Under practical field conditions, the top layer of many soils is often undergoing continued structural, biological, and morphological changes [*Hills and Reynolds*, 1969; *Nielsen et al.*, 1973; *Ritsema and Dekker*, 1995]. These changes, especially when the soil is cultivated, lead to the development of macropores, cracks in fine-textured soils, and earthworm holes and decayed root channels. On the basis of the analysis of the soil water retention curves of 28 different soils, *Bouwer* [1964, p. 4] concluded that because of the occurrence of relatively large

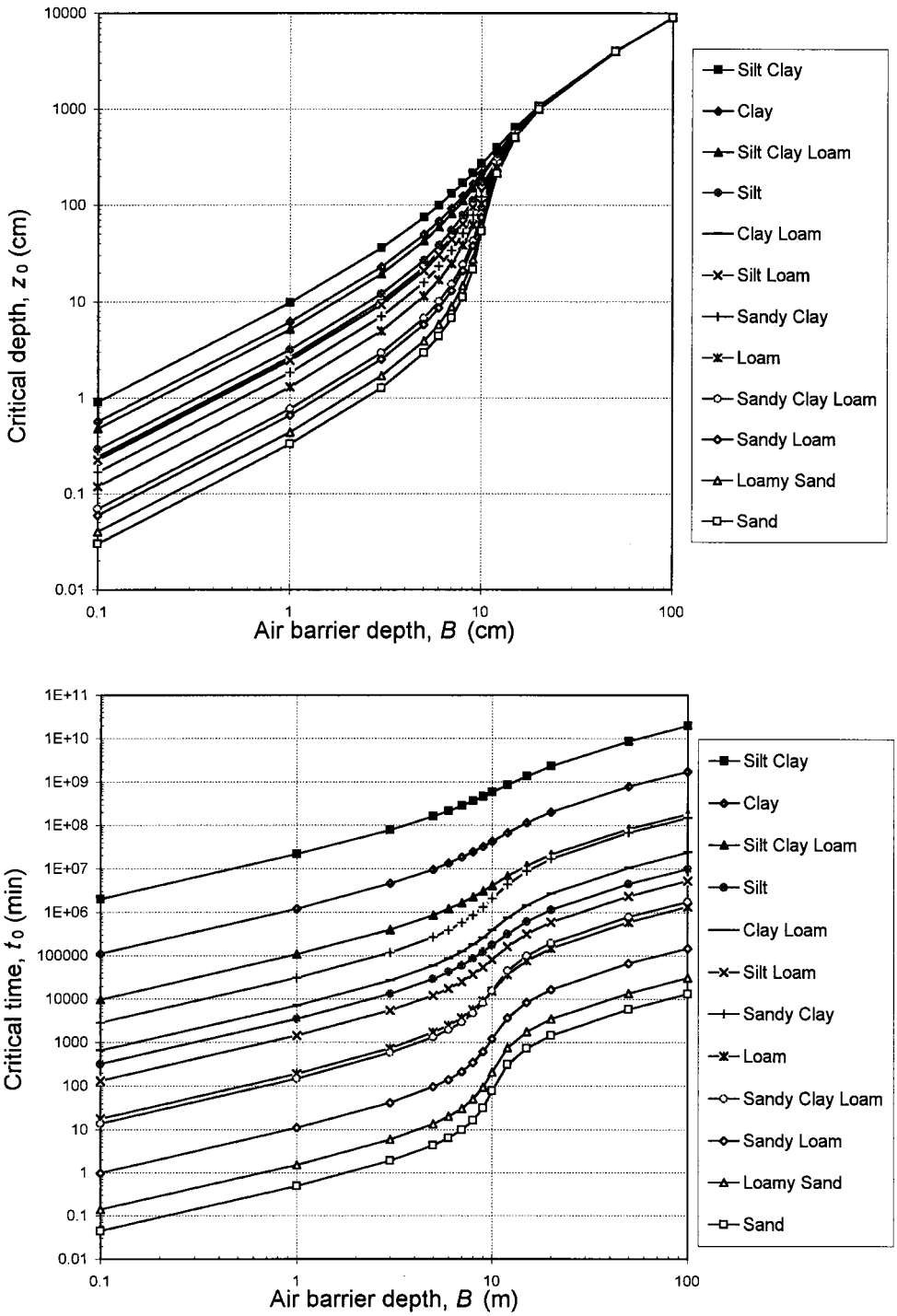

Figure 1. Critical wetting depth (z_0) and corresponding wetting time (t_0) at the zero rate of infiltration with air compression ahead of the wetting front.

pores, "fine textured clay and loamy soils with a well developed structure tend to behave as coarse-textured sandy soils". This suggests that the top few centimeters of a soil often can be treated as if they were sandy soils with relatively large values of K_s and h_{wb}. For such conditions it can be concluded from (16) and (17) or from Figure 1 that z_0 and t_0 are negligible compared with the total depth and duration of an infiltration event. Therefore, from (22), a useful explicit equation for the entire period of infiltration with air compression and counterflow is given by

$$i_w = \frac{1}{2}\,[K_c\phi(1 - S_{w,0} - S_{nw,c})(h_{ab} - h_{wb})]^{1/2}\,t^{-1/2} \quad (23)$$

This equation resembles the *Kostiakov* [1932] equation (i.e., $i_w = kt^{-c}$), where c is now exactly ½,

$$k = \frac{1}{2}\,[K_c\phi(1 - S_{w,0} - S_{nw,c})(h_{ab} - h_{wb})]^{1/2} \quad (24)$$

Equation (23) also resembles the infiltration equation of *Philip* [1957c], $i_w = 0.5St^{-1/2} + A$, where $A = 0$ and the sorptivity, S, is defined by

$$S = [K_c\phi(1 - S_{w,0} - S_{nw,c})(h_{ab} - h_{wb})]^{1/2} \quad (25)$$

With air counterflow from ahead of the wetting front, (23) indicates that the rate of infiltration will decrease continuously with time instead of reaching a steady state constant infiltration rate. Steady state infiltration rates occur only in the case of infiltration without air counterflow as shown by (10) and (11). We emphasize that parameters in (10), (11), (13), (14), (22), and (23) are all physically meaningful, pertaining to basic characteristics of both the porous medium and the wetting and nonwetting fluids (water and air).

Integration of (23) gives the equation for the cumulative water depth of infiltration (I_w):

$$I_w = [K_c\phi(1 - S_{w,0} - S_{nw,c})(h_{ab} - h_{wb})]^{1/2}\, t^{1/2} \quad (26)$$

The functional equations (10), (11), (13), (14), (22), (23), and (26) readily permit the construction of graphical curves relating i_w, I_w, z, and h_{af} with time t. Parameters K_s, K_c, ϕ, $S_{w,0}$, $S_{nw,0}$, $S_{nw,c}$, h_{ab}, and h_{wb} can be determined by means of simple experiments. The determination of k_{rc} value from detailed (static) soil characteristics data was recently summarized by *Morel-Seytoux et al*. [1996]. Experimental data of *Vachaud et al*. [1974] and *Touma et al*. [1984] indicate that the value of k_{rc} should be about 0.5. *Bouwer* [1964] also suggested that for field conditions (air may be confined), $K_c \approx 0.5\ K_s$. An analysis by *Wang et al*. [1997] of these far very few published data indicates that $S_{nw,c}$ is about 7% higher than $S_{nw,0}$ in sandy soils.

Although the above equations apply to homogeneous media, they can be readily extended to nonuniform media. Boyle's perfect gas law shown by (12) is no longer applicable to the nonuniform media. However, (12) affects only the calculation of z_0 and t_0 (which should be very small because of macropores at or near the soil surface). In case of multiple layered media, the parameters ϕ, h_{ab}, h_{wb}, $S_{w,0}$, and $S_{nw,0}$ should all change with z; however, K_s or K_c should be kept at a value corresponding to the most impermeable layer that is being wetted. This most impermeable layer serves as a bottleneck for water infiltrating into the underlying layers.

3. Performance of the Equations

3.1. Theoretical Predictions

We assume a situation where the soil surface is ponded with water to a depth $h_0 = 5$ cm, an air barrier exists at depth $B = 100$ cm, and water is infiltrating into a "sand" and a "clay" soil with hydraulic parameters as shown in Table 1. Results of (13), (14), (22), (23), and (26) for the sand are shown in Figure 2a; close-up view of the infiltration rate i_w as affected by both air compression ($h_{af} < z + h_0 + h_{wb}$) and air counterflow ($h_{af} > z + h_0 + h_{wb}$) is shown in Figure 2b. The confined air pressure $h_{af}(c)$ was calculated from (13) for the initial period of infiltration. After air breakthrough, $h_{af}(c) = h_0 + z + (h_{ab} + h_{wb})/2$, which is the average of the air-breaking and the air-closing values as shown by (3) and (4). Similar results for the clay soil are shown in Figure 3.

For the different input parameters, Table 2 compares the output of (10), (11), (13), (14), (22), (23), and (26) for the two soils. The residual wetting-fluid (water) saturation was given by $S_{w,0} = \theta_r/\theta_s$ (data from Table 1), and the natural residual nonwetting-fluid (air) saturation was assumed to be $S_{nw,0} = S_{w,0}/2$ [*Luckner et al*., 1989]. The residual air saturation with air effect, $S_{nw,c}$, was taken 7% greater than $S_{nw,0}$ and $K_c = 0.5\ K_s$ [*Vachaud et al*., 1974; *Touma et al*., 1984; *Wang et al*., 1997]. The total porosity ϕ was hence determined by the relationship $\phi = \theta_s + \phi S_{nw,0}$ or $\phi = 2\theta_s^2/(2\theta_s - \theta_r)$. Infiltration into the air-confining sand came to an immediate halt ($i_w = 0$) at $z_0 = 0.88$ cm and $t_0 = 1.25$ min. For the clay soil, however, infiltration ceased after a much later time ($t_0 = 1167$ min) at wetting depth $z_0 = 6.7$ cm. Immediately after time t_0, i_w jumps to a relatively high value as shown in Figures 2b and 3b. Compared with the total time of infiltration, $T(o)$, under the open condition ($h_{af} = 0$), the total time of infiltration, $T(c)$, under air-confining condition ($z = B = 100$ cm), increased 46 times (2835/61) in the sand and 6.9 times in the clay. The corresponding final rate of infiltration, $i_w(c)_f$, under the confined condition is reduced to 1.15% in the sand and 10.6% in the clay, relative to the final rates of infiltration, $i_w(o)_f$, under open conditions. Judging from these results, the

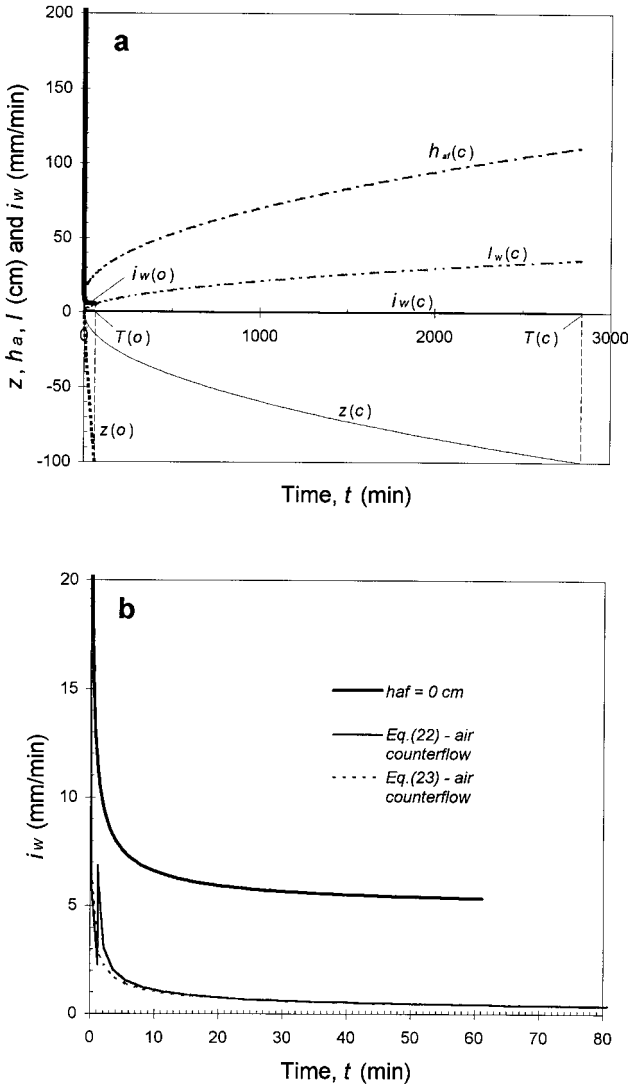

Figure 2. Prediction of equations (10), (11), (13), (14), (22), and (23) for water infiltration into a sand with parameters shown in Table 1 (i_w is the rate of infiltration, z the depth of wetting, h_{af} the gauge air pressure ahead of the wetting front, and T the total time of infiltration at $z = B = 100$ cm; c and o with parenthesis denote the "air confined" condition and the "open" condition, respectively). A close-up view of i_w in Figure 2a is shown in Figure 2b.

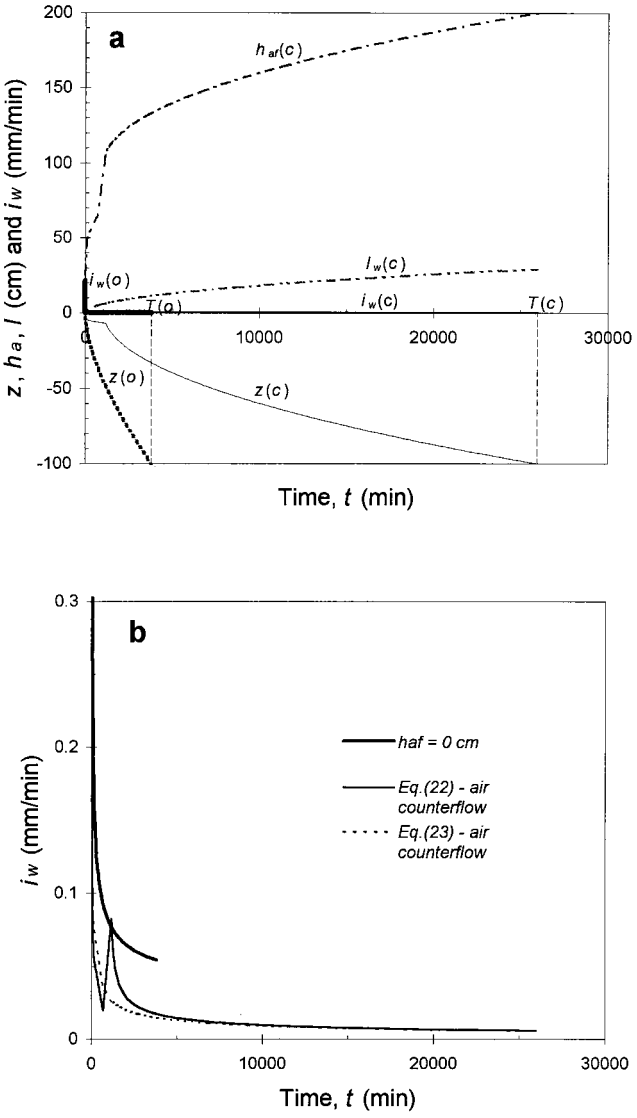

Figure 3. Prediction of equations (10), (11), (13), (14), (22), and (23) for water infiltration into a clay with flow parameters shown in Table 1 (symbols are as defined for Figure 2).

effects of air confinement and counterflow on the rate and duration of infiltration are considerable, being more pronounced in sandy soils than in clay soils. The lower input value of ϕ and higher values of $S_{w,0}$ and $S_{nw,0}$ for the clay soil accounted for the lower value of cumulative infiltration depth, I_f, in the clay.

3.2. Experimental Validation

Laboratory experiments using a transparent cylinder (8.6 cm i.d. and 45 cm sample height) under both air-draining and air-confining conditions were conducted to test the theoretical predictions. Detailed descriptions of the experimental material and procedures are given by *Wang et al*. [1997]. Analysis of the observed soil water characteristic curve of the sand and tension infiltrometer data indicated that the air-bubbling value h_{ab} of the loamy sand was about 21 cm and that the water-bubbling value h_{wb} was about 9 cm. The parameters of *van Genuchten* [1980] retention model with $m = 1 - 1/n$ were $\alpha = 0.053$ cm^{-1}, and $m = 0.705$ [*Wang et al*., 1997]. The total porosity of the sand was $\phi = 0.4$, and the residual water saturation of the oven-dried sand was taken as $S_{w,0} = 0$. Residual air saturation under the air-draining condition was $S_{nw,0} = 0.176$ and under the air-confining condition $S_{nw,c} = 0.305$ [*Wang et al*., 1997]. Repeated experiments using a constant-head permeameter [*Klute and Dirksen*, 1986] resulted in an average water conductivity K_s of 2217 cm/day (1.54 cm/min) without air effects. The natural saturated water content (under air-draining condition) was estimated as $\theta_s = \phi(1 - S_{nw,0}) = 0.4(1 - 0.176) = 0.33$. For the air-confining condition the average water content in the wetted zone was estimated as $\theta_w = \phi(1 - S_{nw,c}) = 0.278$, corresponding to a normalized water content of $\theta^* = \theta_w/\theta_s = 0.8424$. These values resulted in a *van Genuchten* [1980] estimate ($m = 1 - 1/n$) for the relative (static) water conductivity of $k_{rw} = \theta^{*1/2}[1 - (1 - \theta^{*1/m})^m]^2 \equiv 0.4005$, and an air-confining water conductivity $K_c \equiv k_{rw}K_s$ of 888 cm/day (0.6166 cm/min).

A typical set of experimental data and the theoretical predictions of (13), (14), (22), and (23) are plotted in Figure 4. When air was set free to escape ($h_{af} = 0$), the values of $i_w(o)$ and $T(o)$ as well as those of the depth of wetting, $z(o)$, adequately described the experimental data. Similarly, under the air-confining condition, satisfactory agreement existed between $i_w(c)$ and the corresponding data. The duration of infiltration, $T(c)$, was also close to the observed data (a perfect fit was achieved when k_{rw} was taken to be 0.50). However, discrepancies still existed between predictions of $z(c)$, $I_w(c)/f$, $h_{af}(c)$, and the corresponding data. We recorded actually two depths of wetting, $z(c)_{\min}$ and $z(c)_{\max}$, which manifested the presence of fingered flow under the air confining condition. Here $z(c)_{\min}$ denotes the depth of the finger tail and $z(c)_{\max}$ is the depth of the finger tip (observed through the wall of the transparent column). Both $z(c)$ and $h_{af}(c)$ were predicted well during the initial stage of infiltration. However, when, because of fingering, the wetting front extended between $z(c)_{\min}$ and $z(c)_{\max}$, the observed $h_{af}(c)$ was always lower than the predicted $h_{af}(c) = z(c) + h_0 + (h_{ab} + h_{wb})/2$. It is not surprising that the values of h_{ab} and h_{wb} of the top layer

Table 2. Input Parameters and the Output of Equations (10), (11), (13), (14), (22), and (23) for the Sand and the Clay Shown in Table 1

	K_s, cm/min	h_{ab}, cm	h_{wb}, cm	ϕ	$S_{w,0}$	$S_{nw,c}$	z_0, cm	t_0, min	$T(o)$, min	$T(c)$, min	$i_w(o)_f$, mm/min	$i_w(c)_f$, mm/min	I_f, cm
Sand	0.495	8	3	0.45	0.1	0.12	0.88	1.25	61	2835	5.346	0.06187	35.1
Clay	0.003	130	60	0.42	0.16	0.15	6.7	1167	3789	25967	0.0545	0.00578	29.4

Here c and o indicate the "confined" and the "open-bottom" conditions, respectively, and the subscript f denotes the final condition at the wetting depth $z = B = 100$ cm.

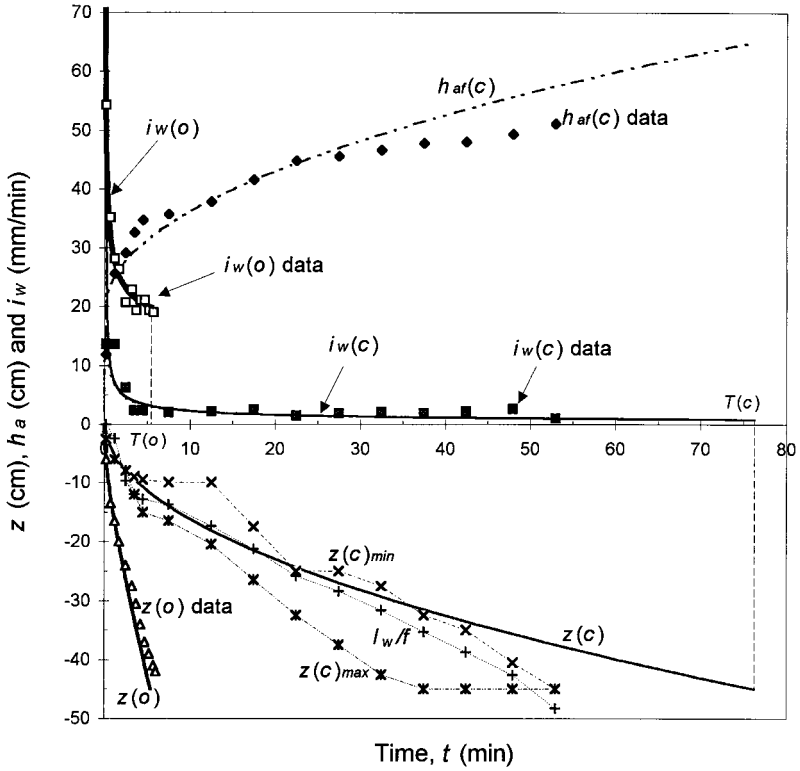

Figure 4. Comparison of observed and predicted infiltration rates in the presence of air compression and air counterflow in a loamy sand (K_s = 2217 cm/day = 1.53 cm/min, h_{ab} = 21 cm, h_{wb} = 9 cm, ϕ = 0.40, $S_{w,0}$ = 0, $S_{nw,0}$ = 0.1, h_0 = 5 cm, and B = 45 cm).

both decreased considerably because of the presence of air channels (macropores) following the eruption of air from the soil surface [*Wang et al*., 1997].

4. Summary and Conclusions

The *Green and Ampt* [1911] equation was extended to include the potential effects of air compression and air counterflow during water infiltration into a porous medium. The capillary pressure at the wetting front was found to vary between the dynamic water-bubbling value and the air-bubbling value of the material when air counterflow occurred from ahead of the wetting front.

Functional infiltration equations accounting for air compression, air counterflow, and flow hysteresis in the porous media were presented. Parameters in the equations are all physically meaningful and readily obtained from laboratory and/or field experiments. Experimental validation showed that the equations remained relatively accurate.

Air compression ahead of the wetting front is a major cause of wetting front instability followed by fingering [*Peck*, 1965b; *Raats*, 1973; *Philip*, 1975; *Wang et al*., 1997]. These processes may substantially affect the rate of water infiltration.

Acknowledgments. This research project was funded by the Katholieke Universiteit Leuven (K. U. Leuven). Comments made by three anonymous reviewers were greatly appreciated.

References

Adrian, D. D., and J. B. Franzini, Impedance to infiltration by pressure build up ahead of the wetting front, *J. Geophys. Res*., *71*(24), 5857–5862, 1966.

Bouwer, H., Unsaturated flow in ground-water hydraulics, *J. Hydraul. Div. Am. Soc. Civ. Eng*., *90*, 121–144, 1964.

Brakensiek, D. L., Estimating the effective capillary pressure in the Green and Ampt infiltration equation, *Water Resour. Res*., *13*(3), 680–682, 1977.

Brooks, R. H., and A. T. Corey, Properties of porous media affecting fluid flow, *J. Irrig. Drain. Div. Am. Soc. Civ. Eng*., *92*, 61–88, 1966.

Brustkern, R. L., and H. J. Morel-Seytoux, Analytical Treatment of two-phase infiltration, *J. Hydraul. Div. Am. Soc. Civ. Eng*., *96*, 2535–2548, 1970.

Brustkern, R. L., and H. J. Morel-Seytoux, Description of water and air movements during infiltration, *J. Hydrol*., *24*, 21–35, 1975.

Carsel, R. F., and R. S. Parrish, Developing joint probability distributions of soil water retention characteristics, *Water Resour. Res*., *24*, 755–769, 1988.

Christiansen, J. E., Effects of entrapped air upon the permeability of soils, *Soil Sci*., *58*, 355–366, 1944.

Corey, A. T., and R. H. Brooks, Drainage Characteristics of soils, *Soil Sci. Soc. Am. Proc*., *39*, 251–255, 1975.

Dixon, R. M., and D. R. Linden, Soil air pressure and water infiltration under border irrigation, *Soil Sci. Soc. Am. Proc*., *36*, 948–953, 1972.

Elrick, D. E., and W. D. Reynolds, Infiltration from constant-head well permeameters and infiltrometers, in *Advances in Measurement of Soil Physical Properties: Brining Theory into Practice*, *SSSA Spec. Publ*., *30*, pp. 1–24, 1992.

Fallow, D. J., and D. E. Elrick, Field measurement of air-entry and water-entry soil water pressure heads, *Soil Sci. Soc. Am. J*., *60*, 1036–1039, 1996.

Felton, G. K., and D. L. Reddell, A Finite element axisymmetrical and

linear model of two-phase flow through porous media, *Trans. ASAE*, *35*(5), 1419–1429, 1992.
Green, W. H., and C. A. Ampt, Studies on soil physics, 1, Flow of air and water through soils, *J. Agric. Sci*., *4*, 1–24, 1911.
Grismer, M. E., M. N. Orang, V. Clausnitzer, and K. Kinney, Effects of air compression and counterflow on infiltration into soils, *J. Irrig. Drain. Eng*., *120*, 775–795, 1994.
Hills, R. C., and S. G. Reynolds, Illustration of soil moisture variability in selected areas and plots of different sizes, *J. Hydrol*., *8*, 27–47, 1969.
Klute, A., and C. Dirksen, Hydraulic conductivity and Diffusivity: Laboratory methods, *Methods of Soil Analysis*, edited by A. Klute, pp. 687–732, Am. Soc. of Agron., Madison, Wis., 1986.
Kostiakov, A. H., On the dynamics of the coefficient of water percolation in soils and on the necessity of studying it from a dynamic point of view for purpose of amelioration, *Transactions 6th Congress of the International Society of Soil Science, Moscow, Russia*, *Part A*, 7–21, 1932.
Latifi, H., S. N. Prasad, and O. J. Helweg, Air entrapment and water infiltration in two-layered soil column, *J. Irrig. Drain. Eng*., *120*, 871–891, 1994.
Luckner, L., M. T. van Genuchten, and D. R. Nielsen, A consistent set of parametric models for the two-phase flow of immiscible fluids in the subsurface, *Water Resour. Res*., *25*, 2187–2193, 1989.
McWhorter, D. B., Infiltration affected by flow of air, *Hydrol. Pap. 49*, Colo. State Univ., Fort Collins, 1971.
Mein, R. G., and C. L. Larson, Modeling infiltration during a steady rain, *Water Resour. Res*., *9*, 384–394, 1973.
Morel-Seytoux, H. J., Two-phase flow in porous media, in *Advances in Hydroscience*, edited by V. T. Chow, pp. 119–202, Academic, San Diego, Calif., 1973.
Morel-Seytoux, H. J., and J. A. Billica, A two-phase numerical model for prediction of infiltration: application to a semi-infinite soil column, *Water Resour. Res*., *21*, 607–615, 1985a.
Morel-Seytoux, H. J., and J. A. Billica, A two-phase numerical model for prediction of infiltration: Case of an impervious bottom, *Water Resour. Res*., *21*, 1389–1396, 1985b.
Morel-Seytoux, H. J., and J. Khanji, Derivation of an equation of infiltration, *Water Resour. Res*., *10*, 795–800, 1974.
Morel-Seytoux, H. J., and J. Khanji, Equation of infiltration with compression and counterflow effects, *Hydro. Sci. J*., *20*, 505–517, 1975.
Morel-Seytoux, H. J., P. D. Meyer, M. Nachabe, J. Touma, M. T. van Genuchten, and R. J. Lenhard, Parameter equivalence for Brooks-Corey and van Genuchten soil Characteristics: Preserving the effective capillary drive, *Water Resour. Res*., *32*(5), 1251–1258, 1996.
Nielsen, D. R., J. W. Biggar, and K. T. Erh, Spatial variability of field measured soil water properties, *Hilgardia*, *42*, 215–260, 1973.
Noblanc, A., and H. J. Morel-Seytoux, Perturbation analysis of two-phase infiltration, *J. Hydraul. Div. Am. Soc. Civ. Eng*., *98*, 1527–1541, 1972.
Parlange, J.-Y., Theory of water movement in soils, 1, One-dimensional absorption, *Soil Sci*., *111*, 134–137, 1971.
Parlange, J.-Y., Theory of water movement in soils, 11, Conclusion and discussion of some recent developments, *Soil Sci*., *119*, 158–161, 1975a.
Parlange, J.-Y., On solving the flow equation in unsaturated soils by optimization: Horizontal infiltration, *Soil Sci. Soc. Am. Proc*., *39*, 415–418, 1975b.
Parlange, J. Y., and D. E. Hill, Air and water movement in porous media: Compressibility effects, *Soil Sci*., *127*, 257–263, 1979.
Peck, A. J., Moisture profile development and air compression during water uptake by bounded porous bodies, 2, Horizontal columns, *Soil Sci*., *99*, 327–334, 1965a.
Peck, A. J., Moisture profile development and air compression during water uptake by bounded porous bodies, 3, Vertical columns, *Soil Sci*., *100*, 44–51, 1965b.
Philip, J. R., The theory of infiltration, 1, The infiltration equation and its solution, *Soil Sci*., *83*, 345–357, 1957a.
Philip, J. R., The theory of infiltration, 2, The profile of infinity, *Soil Sci*., *83*, 435–448, 1957b.
Philip, J. R., The theory of infiltration, 3, Moisture profiles and relation to experiment, *Soil Sci*., *84*, 163–178, 1957c.
Philip, J. R., The theory of infiltration, 4, Sorptivity and algebraic infiltration equations, *Soil Sci*., *84*, 257–263, 1957d.
Philip, J. R., The growth of disturbance in unstable infiltration flow, *Soil Sci. Soc. Am. Proc*., *39*, 1049–1053, 1975.
Philip, J. R., Variable head ponded infiltration under constant or variable rainfall, *Water Resour. Res*., *29*, 2155–2165, 1993.
Powers, W. L., Soil-water movement as affected by confined air, *J. Agric. Res*., *49*, 1125–1134, 1934.
Raats, P. A. C., Unstable wetting fronts in uniform and non-uniform soils, *Soil Sci. Soc. Am. Proc*., *37*, 681–685, 1973.
Ritsema, C. J., and L. W. Dekker, Distribution flow: A general process in the top layer of water repellent soils, *Water Resour. Res*., *31*, 1187–1200, 1995.
Sander, G. C., J.-Y. Parlange, and W. L. Hogarth, Air and water flow, II, Gravitational flow with an arbitrary flux boundary condition, *J. Hydrol*., *99*, 225–234, 1988.
Smiles, D. E., G. Vachaud, and M. Vauclin, A test of the uniqueness of the soil moisture characteristics during transient, non hysteretic flow of water in a rigid soil, *Soil Sci. Soc. Am. Proc*., *35*, 534–539, 1971.
Sonu, J., and H. J. Morel-Seytoux, Water and air movement in a bounded deep homogeneous soil, *J. Hydrol*., *29*, 23–42, 1976.
Touma, J., G. Vachaud, and J.-Y. Parlange, Air and water flow in a sealed, ponded vertical soil column: Experiment and model, *Soil Sci*., *137*, 181–187, 1984.
Vachaud, G., M. Vauclin, D. Khanji, and M. Wakil, Effects of air pressure on water flow in an unsaturated stratified vertical column of sand, *Water Resour. Res*., *9*, 160–173, 1973.
Vachaud, G., J. P. Gaudet, and V. Kuraz, Air and water flow during ponded infiltration in a bounded column of soil, *J. Hydrol*., *22*, 89–108, 1974.
van Genuchten, M. T., A closed form equation for predicting the hydraulic conductivity of unsaturated soils, *Soil Sci. Soc. Am. J*., *44*, 892–898, 1980.
van Genuchten, M. T., F. J. Leij, and S. R. Yates, The RETC Code for quantifying the hydraulic functions of unsaturated soils, U.S. Salinity Laboratory, U.S. Dep. of Agric., Agric. Res. Serv., Riverside, Calif., 1991.
Wang, Z., J. Feyen, D. R. Nielsen, and M. T. van Genuchten, Air entrapment effects on infiltration rate and flow instability, *Water Resour. Res*., in press, 1997.
Watson, K. K., and A. A. Curtis, The use of a transformed boundary condition in modeling air compression during infiltration, *Soil Sci. Soc. Am. J*., *43*, 848–850, 1979.
Whisler, F. D., and H. Bouwer, Comparison of methods for calculating vertical drainage and infiltration for soils, *J. Hydrol*., *10*(1), 1–9, 1970.
Wilson, L. G., and J. N. Luthin, Effects of air flow ahead of the wetting front on infiltration, *Soil Sci*., *91*, 137–143, 1963.
Youngs, E. G., and A. J. Peck, Moisture profile development and air compression during water uptake by bounded porous bodies, 1, Theoretical introduction, *Soil Sci*., *98*, 290–294, 1964.

J. Feyen and Z. Wang, Institute for Land and Water Management, Katholieke Universiteit Leuven, Vital Decosterstraat 102, 3000 Leuven, Belgium. (e-mail: zhi.wang@agr.kuleuven.ac.be)
D. R. Nielsen, Department of Land, Air, and Water Resources, University of California, Davis, CA 95616.
M. T. van Genuchten, U.S. Salinity Laboratory, USDA-ARS, 450 W. Big Springs Rd., Riverside, CA 92507-4617.

(Received December 18, 1996; revised May 20, 1997;
accepted June 8, 1997.)